Aqueous Chemical Solution Deposition of Ferroelectric Ti^{4+} Cosubstituted $(Bi,La)_4Ti_3O_{12}$ Thin Films

An Hardy,[†] Jan D'Haen,[‡,§] Ludovic Goux,[||] Dirk Wouters,[||] Marlies Van Bael,[†,‡] Heidi Van den Rul,[‡] and Jules Mullens*[,†]

Hasselt University, Institute for Materials Research, Laboratory of Inorganic and Physical Chemistry and Materials Physics, B-3590 Diepenbeek, Belgium, IMEC VZW, Division IMOMEC, B-3590 Diepenbeek, Belgium, and IMEC VZW, B-3001 Heverlee-Leuven, Belgium

Received January 11, 2007. Revised Manuscript Received March 28, 2007

A new, entirely aqueous method for the deposition of ferroelectric lanthanum substituted bismuth titanate including cosubstitution of Ti^{4+} with higher valent metal ions (W^{6+}, Mo^{6+}, Nb^{5+}, and V^{5+}) is presented. The strong tendency toward hydrolysis and condensation of highly valent metal ions, causing precipitation of (oxy)hydroxides, was adequately prevented by new synthesis routes for stable, aqueous (mono)metal ion precursor solutions based on citratoperoxo or nitrilotriacetatoperoxo complexes. The (mono)metal ion precursors are optimized for convenient mixing into multimetal ion precursors with the desired composition, which are deposited using spin-coating. The effect of the La^{3+} content as well as the different cosubstitutions on the films' ferroelectric remanent polarization, crystalline, and microstructural properties was studied. A maximal $2P_r$ value of 17.2 $\mu C/cm^2$ was obtained for the $Bi_{3.5}La_{0.5}Ti_{2.97}V_{0.03}O_{12+\delta}$ thin film after annealing at a temperature as low as 650 °C. The cosubstituting metal ions affect both the crystallographic orientation and the grain growth behavior of the BLTM thin films. A reduction of the *c*-axis preferential orientation and an enhanced grain growth correlate with improved remanent polarization. The general potential of this original aqueous route is two-fold: synthesis of even highly complex multimetal oxide compositions is accomplished easily at low temperatures and a strong ecologic and economic advantage over solvent-based chemical routes is obtained.

Introduction

Bismuth titanate is a lead-free, ferroelectric material with a layered perovskite structure consisting of alternating $Bi_2O_2^{2+}$ layers and $Bi_2Ti_3O_{10}^{2-}$ pseudo-perovskite blocks, which is considered for application in nonvolatile ferroelectric random access memories. It is characterized by a very large spontaneous polarization along the *a*-axis (∼50 $\mu C/cm^2$ for a single crystal[1]), unlike $SrBi_2Ta_2O_9$ (∼15 $\mu C/cm^2$), which is also lead-free and considered for the same application. High remanent polarization (P_r) values are necessary to maintain a detectable signal even with thorough miniaturization of the memory cells. Unfortunately, bismuth titanate (BiT) itself suffers from fatigue, a reduction of the P_r as the amount of switching cycles is increased. By partially substituting Bi^{3+} with La^{3+}, the fatigue properties are greatly improved, however.[2] Further strategies are being developed to improve the ferroelectric characteristics even at relatively low processing temperatures. One way is to selectively control both the A-site and the B-site substitution in BiT: by substituting both the Ti^{4+} ions with higher valent transition metal ions and the Bi^{3+} with La^{3+} ions, the P_r value is expected to increase, while maintaining a good fatigue resistance. An explanation for the cosubstitution effect is the reduction of the number of oxygen vacancies upon incorporation of higher valent metal ions, leading to reduced domain pinning and a higher remanent polarization.[3]

In the presented work, this concept is applied to the fabrication of layered perovskite thin films deposited by means of an original, entirely aqueous solution−gel route. Unlike normal sol−gel techniques,[4] in which organic solvents are used that lead to reproductive hazards (2-methoxyethanol, 2-ethoxyethanol), carcinogenic effects (benzene), or neurotoxic effects (*n*-hexane), the use of water as the solvent implies a reduction of environmental and safety hazards while at the same time providing an inexpensive alternative to other chemical solution deposition (CSD) methods.[5,6] In our laboratory, the aqueous solution−gel method was applied to the preparation of bulk metal oxides[7−13] as well as thin films.[14−16] In the present study, new synthesis routes for

* Corresponding author. Tel.: 0032 (0)11 26 83 93; fax: 0032 (0)11 26 83 23; e-mail: jules.mullens@uhasselt.be.
[†] Hasselt University, Institute for Materials Research, Laboratory of Inorganic and Physical Chemistry.
[‡] IMEC VZW, Division IMOMEC.
[§] Hasselt University, Institute for Materials Research, Materials Physics.
[||] IMEC VZW.

(1) Cummins, S. E.; Cross, L. E. *J. Appl. Phys.* **1968**, *39*, 2268.
(2) Park, B. H.; Kang, B. S.; Bu, S. D.; Noh, T. W.; Lee, J.; Jo, W. *Nature* **1999**, *401*, 682.
(3) Noguchi, Y.; Miwa, I.; Goshima, Y.; Miyayama, M. *Jpn. J. Appl. Phys.* **2000**, *39*, 1259.
(4) Schwartz, R. W.; Schneller, T.; Waser, R. *C. R. Chim.* **2004**, *7*, 433.
(5) Kakihana, M.; Szanics, J.; Tada, M. *Bull. Korean Chem. Soc.* **1999**, *20*, 893.
(6) Narendar, Y. Regulating oxide crystallization from Pb, Mg, Nb-carboxylate gels. Ph.D. Thesis, Pennsylvania State University, University Park, Pennsylvania, 1996.
(7) Pagnaer, J.; Hardy, A.; Mondelaers, D.; Vanhoyland, G.; D'Haen, J.; Van Bael, M. K.; Van den Rul, H.; Mullens, J.; Van Poucke, L. C. *Mater. Sci. Eng., B* **2005**, *118*, 79.
(8) Storms, A.; Van Bael, M. K.; Van den Rul, H.; Vanhoyland, G.; Mullens, J.; Van Poucke, L. C. *Key Eng. Mater.* **2004**, *264−268*, 347.

10.1021/cm070101x CCC: $37.00 © 2007 American Chemical Society
Published on Web 05/10/2007

aqueous precursor solutions of highly valent metal ions are reported, as well as their application to the preparation of aqueous multimetal ion precursor solutions. The latter are used to deposit lanthanum substituted bismuth titanate thin films cosubstituted with higher valent metal ions, BLTM ($(Bi,La)_4(Ti,M)_3O_{12}$, $M^{n+} = W^{6+}$, Mo^{6+}, V^{5+}, or Nb^{5+}). The effect of the (co-)substitution on the films' ferroelectric remanent polarization is explained based on microstructural and crystallographic characterization.

Experimental Procedures

Precursor Preparation and Materials. To prepare the BLTM precursors, aqueous M^{n+} ($M^{n+} = Bi^{3+}$, La^{3+}, Ti^{4+}, W^{6+}, Mo^{6+}, V^{5+}, or Nb^{5+}) solutions were synthesized for each of the individual metal ions.

The synthesis of aqueous Bi^{3+}, La^{3+}, Ti^{4+}, and Nb^{5+} (pH = 7.5) solutions is carried out as reported recently.[15,17,18] Bismuth and lanthanum citrate, either commercially available or synthesized from the oxide by reaction with citric acid, were dissolved in water by the addition of ammonia and stabilized using monoethanolamine. Titanium(IV) and niobium(V) citratoperoxo complexes were synthesized by refluxing selected starting products, either freshly hydrolyzed Ti(IV)isopropoxide or ammonium niobiumoxalate, with hydrogen peroxide and citric acid, followed by pH adjustment with NH_3 (to pH = 7,5) and a second reflux step.

New synthetic routes are presented here for the preparation of aqueous W^{6+}, Mo^{6+}, and V^{5+} solutions (Figure 1). The starting products are ammonium metatungstate hydrate (AMT, $(NH_4)_6W_{12}O_{39}$, 99.99%, Aldrich), ammonium heptamolybdate tetrahydrate (AMD, $(NH_4)_6Mo_7O_{24}{\cdot}4H_2O$, 99.3−101.8% Merck), and ammonium metavanadate (NH_4VO_3, 99+%, Aldrich). Citric acid ($C_6H_8O_7$, Aldrich, 99%) or nitrilotriacetic acid ($C_6H_9NO_6$, Acros, 99%) and hydrogen peroxide (H_2O_2, stabilized, Acros, 35% aqueous solution) were used as complexing agents. The pH was controlled using ammonia (NH_3, Merck, 32% aqueous solution, extra pure).

The (mono)metal ion solutions were mixed in the desired stoichiometry. To this end, their exact concentration was determined using ICP-AES (PerkinElmer, Optima 3000). The BLT(M) precursor solutions were prepared with a Bi excess of 10 mol % to compensate for Bi^{3+} loss during thermal treatment of the films and to maximize the remanent polarization (P_r).[16] Two different La^{3+} contents, 0.5 and 0.8 mol %, were studied. The selected compositions were $Bi_{4-x}La_xTi_{2.97}M_{0.03}O_{12+\delta}$ with $x = 0.5$ ($BL_{0.5}TM$) or $x = 0.8$ ($BL_{0.8}TM$) and with $M^{n+} = Mo^{6+}$, W^{6+}, Nb^{5+}, or V^{5+}.[19−25]

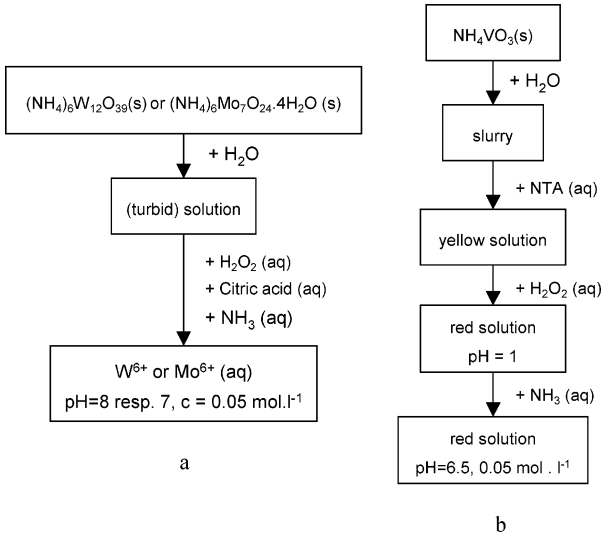

Figure 1. Schematic preparation of the W^{6+}, Mo^{6+}, and V^{5+} aqueous precursor solutions.

Thin Film Deposition by Spin-Coating. Thin films were deposited by spin-coating in a clean room environment onto SPM/APM cleaned[26] platinized silicon wafers and were subsequently heat treated on three hot plates at 160 °C/1′, 260 °C/2′, and 480 °C/2′. Finally, each layer was immediately crystallized in a rapid thermal processing furnace at 650 °C (700 °C, respectively) for 30 s, with a heating rate of 50 °C/s in oxygen. After repeating the coating process three times, to obtain a total film thickness of ∼120 nm, the film was subjected to a final crystallization step at 650 °C (700 °C, respectively) for 30 min in oxygen, with a heating rate of 10 °C/s. The thermal budget was limited, as it is important in view of FRAM integration to maintain annealing temperatures below 650−700 °C.[27]

Characterization Methods. The remanent polarization (P_r) values of the films were determined from measurements of the ferroelectric hysteresis loops using a modified Sawyer−Tower circuit (triangular signal 1 kHz, amplitudes 1−5 V). The crystal structure was studied by coupled $\theta-2\theta$ X-ray diffraction (XRD) measurements on a Siemens D-5000 diffractometer with a Cu Kα radiation source and a scintillation detector, using a step size of 0.04°2θ, counting 2.5 s per step. Thin film morphology and microstructure were characterized by means of scanning electron microscopy (FEI Quanta 200 FEG) with an acceleration voltage of 10 kV.

(9) Nelis, D.; Mondelaers, D.; Vanhoyland, G.; Hardy, A.; Van Werde, K.; Van den Rul, H.; Van Bael, M. K.; Mullens, J.; Van Poucke, L. C.; D'Haen, J. *Thermochim. Acta* **2005**, *426*, 39.
(10) Van den Rul, H.; Mondelaers, D.; Van Bael, M. K.; Mullens, J. *J. Sol-Gel Sci. Technol.* **2006**, *39*, 41.
(11) Van Werde, K.; Vanhoyland, G.; Mondelaers, D.; Van den Rul, H.; Van Bael, M.; Mullens, J.; Van Poucke, L. *J. Mater. Sci.* **2007**, *42*, 624.
(12) Geuzens, E.; Vanhoyland, G.; D'Haen, J.; Van Bael, M. K.; Van den Rul, H.; Mullens, J.; Van Poucke, L. C. *Key Eng. Mater.* **2004**, *264−268*, 343.
(13) Truijen, I.; Van Bael, M. K.; Van den Rul, H.; D'Haen, J.; Mullens, J. *J. Sol-Gel Sci. Technol.* **2007**, *41*, 43.
(14) Hardy, A.; Nelis, D.; Vanhoyland, G.; Van Bael, M. K.; Van den Rul, H.; Mullens, J.; Van Poucke, L. C.; D'Haen, J.; Goux, L.; Wouters, D. J. *Thin Solid Films* **2005**, *492*, 105.
(15) Hardy, A.; Nelis, D.; Vanhoyland, G.; Van Bael, M. K.; Van den Rul, H.; Mullens, J.; Van Poucke, L. C.; D'Haen, J.; Goux, L.; Wouters, D. J. *Mater. Chem. Phys.* **2005**, *92*, 431.
(16) Hardy, A.; Nelis, D.; Vanhoyland, G.; van Bael, M. K.; Mullens, J.; van Poucke, L. C.; D'Haen, J.; Wouters, D. J. *Integr. Ferroelectr.* **2004**, *62*, 205.
(17) Narendar, Y.; Messing, G. L. *Chem. Mater.* **1997**, *9*, 580.
(18) Nelis, D.; Van Werde, K.; Mondelaers, D.; Vanhoyland, G.; Van den Rul, H.; Van Bael, M. K.; Mullens, J.; Van Poucke, L. C. *J. Sol-Gel Sci. Technol.* **2003**, *26*, 1125.
(19) Watanabe, T.; Kojima, T.; Sakai, T.; Funakubo, H.; Osada, M.; Noguchi, Y.; Miyayama, M. *J. Appl. Phys.* **2002**, *92*, 1518.
(20) Ohki, H.; Wang, X. S.; Ishiwara, H. *Jpn. J. Appl. Phys.* **2005**, *44*, 964.
(21) Singh, S. K.; Ishiwara, H. *Thin Solid Films* **2006**, *497*, 90.
(22) Chaudhuri, A. R.; Laha, A.; Krupanidhi, S. B. *Solid State Commun.* **2005**, *133*, 611.
(23) Wang, X. S.; Ishiwara, H. *Appl. Phys. Lett.* **2003**, *82*, 2479.
(24) Funakubo, H.; Watanabe, T.; Kojima, T.; Sakai, T.; Noguchi, Y.; Miyayama, M.; Osada, M.; Kakihana, M.; Saito, K. *J. Cryst. Growth* **2003**, *248*, 180.
(25) Hardy, A.; Vanhoyland, G.; Van Genechten, D.; Van Bael, M.; Van den Rul, H.; Mullens, J.; D'Haen, J.; Goux, L.; Wouters, D. J. *J. Sol-Gel Sci. Technol.* **2007**, *42*, 239.
(26) Van Bael, M. K.; Nelis, D.; Hardy, A.; Mondelaers, D.; Van Werde, K.; D'Haen, J.; Vanhoyland, G.; Van den Rul, H.; Mullens, J.; Van Poucke, L. C.; Frederix, F.; Wouters, D. J. *Integr. Ferroelectr.* **2002**, *45*, 113.
(27) Waser Ed., R., Ed. *Nanoelectronics and Information Technology—Advanced Electronic Materials and Novel Devices*; Wiley-VCH Verlag GmbH and Co.: Weinheim, 2003.

Results

Precursor Synthesis. W^{6+} and Mo^{6+} precursors (Figure 1a) were based on complexation with hydrogen peroxide and citrates. The starting products (AMT and AMD, respectively) were selected to obtain the pure metal oxide after thermal decomposition, avoiding contamination of the final BLTM oxide with nonvolatile counterions. AMT was dissolved in a small amount of water, while AMD was mixed with water, but it did not dissolve completely. Hydrogen peroxide and citric acid were added in a molar ratio of 1.1:1 and 2:1 M^{6+}, respectively, analogous to the preparation of the stable Ti^{4+} precursor solution. The pH was subsequently raised by the addition of ammonia (32%, Merck) to pH = 7 or 8 (Figure 1a). In this way, clear and stable solutions were obtained. For practical reasons, the solutions were prepared in a very low concentration (0.05 mol L^{-1}), as only very small amounts of Ti^{4+} have to be substituted by these metal ions.

The preparation of a precursor solution for V^{5+} based on a citrato complex was studied as well. However, the addition of H_2O_2 and citric acid to a slurry of ammonium metavanadate in water was unsuccessful: the evolution of a gas, precipication of a solid, and subsequent changes in color were observed. Therefore, the synthesis route was adjusted by applying a different complexing agent. The starting product was still ammonium metavanadate (NH_4VO_3). It was mixed with water to obtain a slurry in the reaction medium. Subsequently, a suspension of nitrilotriacetic acid (NTA) in water was added in a molar ratio of 1.25:1 V^{5+}. A bright yellow solution was formed, which still contained undissolved particles, however. H_2O_2 was added to this mixture in a molar ratio of 3:1 V^{5+}. In this way, a dark red solution with pH = 1, containing undissolved particles, was obtained. Finally, the pH was raised to 6.5 with NH_3(aq), which produced a completely clear, red solution. This solution remained stable for at least a year: no precipitation or color change was observed. Even when citric acid was added to these solutions, they remained stable, which is important since the vanadium(V) complex will be mixed with excess citrates when the BLTV precursor solution is prepared by mixing the (mono)metal ion precursors. Furthermore, the V(V) stability during evaporation of the solution and thermal decomposition was checked. The V(V) precursor can be evaporated in a Petri dish at 60 °C in a furnace to form a clear gel, without precipitation. Color changes, indicating a reduction of V(V), are bypassed if the time in the furnace is limited to the minimum for gelation (1.5 h). To verify that V(V) is not reduced during thermal decomposition of the nitrilotriacetatoperoxovanadate(V) gel either, the gel was heated to 600 °C for complete decomposition (10 °C/min, 100 mL/min dry air). An XRD pattern (Figure 2) of the product shows that at 600 °C, pure V_2O_5 is formed.

Thin Film Characterization. Ferroelectric Hysteresis Loops. The ferroelectric P−E hysteresis loops of the $BL_{0.8}$TM films are shown in Figure 3. The P_r values obtained at an amplitude of 5 V for the films crystallized at 650 °C are summarized in Table 1. At 650 °C, substitution with Nb^{5+} and V^{5+} leads to a strong improvement of the ferroelectric P_r. For $BL_{0.8}$TNb a P_r value of 5.6 μC/cm^2 and for $BL_{0.8}$TV a high P_r value of 7.0 μC/cm^2 were obtained as compared

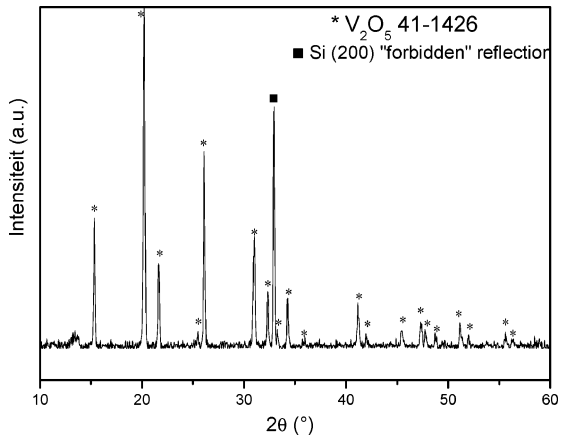

Figure 2. XRD pattern of the nitrilotriacetatoperoxo-V(V)-gel after heat treatment at 600 °C in dry air.

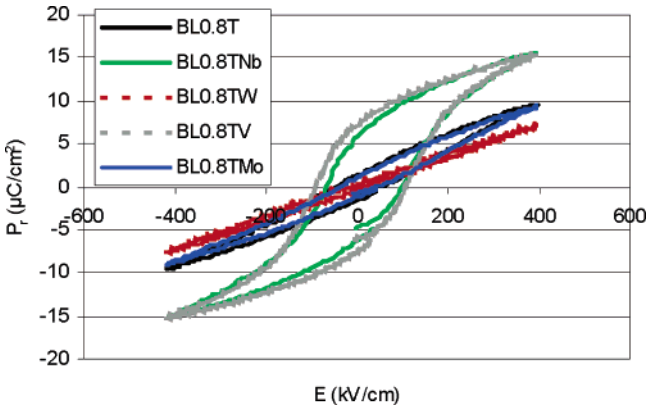

Figure 3. Ferroelectric hysteresis loops at 5 V amplitude of $BL_{0.8}$TM thin films crystallized at 650 °C.

Table 1. Comparison of Remanent Polarization at 5 V of Bl_xTM Thin Films Crystallized at 650 °C

	P_r ($\mu C/cm^2$)		P_r ($\mu C/cm^2$)
$BL_{0.8}$TW	0.2	$BL_{0.5}$TW	4.2
$BL_{0.8}$TMo	1.3	$BL_{0.5}$TMo	5.6
$BL_{0.8}$T	1.3	$BL_{0.5}$T	6.1
$BL_{0.8}$TNb	5.6	$BL_{0.5}$TNb	6.8
$BL_{0.8}$TV	7.0	$BL_{0.5}$TV	8.6

to P_r = 1.3 μC/cm^2 for the $BL_{0.8}$T film without cosubstitution. Substitution with Mo^{6+} is shown to have no effect on the remanent polarization: the $BL_{0.8}$TMo film also showed a P_r value of 1.3 μC/cm^2. W^{6+} had an adverse effect on the ferroelectric property: the $BL_{0.8}$TW film shows almost no hysteresis behavior (0.2 μC/cm^2). After crystallization at 700 °C, the trend remains the same as at 650 °C, but the P_r values increase for all BLTM compositions (e.g., the P_r value of undoped $BL_{0.8}$T was improved to a value of 4.0 μC/cm^2). The $BL_{0.8}$TW film that was crystallized at 700 °C now also showed clear hysteresis behavior with a P_r value of 3.1 μC/cm^2, which is still lower than that of non-cosubstituted $BL_{0.8}$T, however.

The ferroelectric hysteresis loops for $BL_{0.5}$TM are shown in Figure 4. The remanent polarization measured at an amplitude of 5 V is summarized for these films in Table 1. Again, after doping $BL_{0.5}$T with Nb^{5+} or V^{5+}, there is a significant increase of the remanent polarization value. The P_r value at 5 V was 6.8 and 8.6 μC/cm^2 for $BL_{0.5}$TNb and $BL_{0.5}$TV, respectively, as compared to a P_r value of 6.1 μC/cm^2 without cosubstitution of Ti^{4+}. Substitution with both

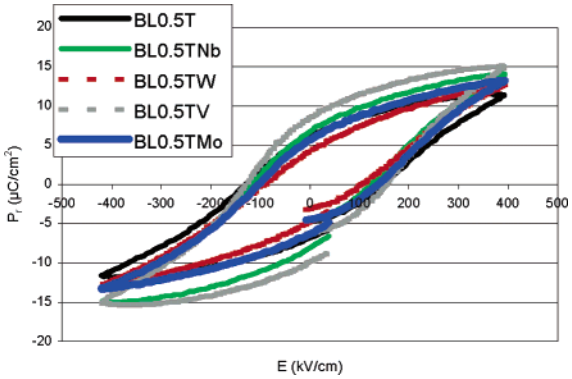

Figure 4. Ferroelectric hysteresis loops at 5 V amplitude of $BL_{0.5}TM$ thin films crystallized at 650 °C.

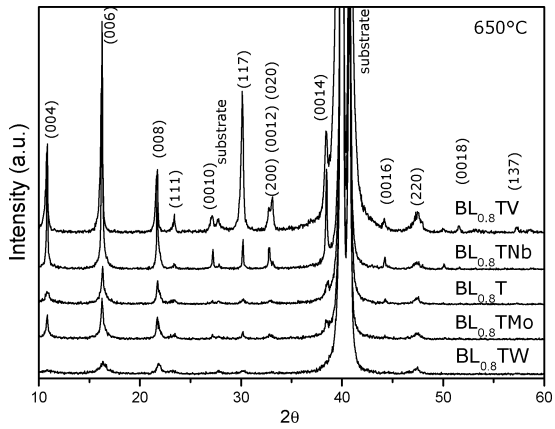

Figure 5. X-ray diffraction patterns of $BL_{0.8}TM$ thin films crystallized at 650 °C.

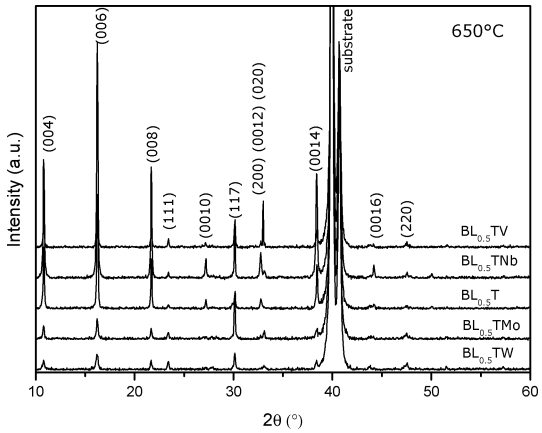

Figure 6. X-ray diffraction patterns of $BL_{0.5}TM$ thin films crystallized at 650 °C.

Mo^{6+} and W^{6+} leads to a reduction of the P_r value, to 5.6 and 4.2 $\mu C/cm^2$, respectively.

Crystal Structure: X-ray Diffraction. The XRD patterns are shown in Figure 5 for the $BL_{0.8}TM$ thin films and in Figure 6 for the $BL_{0.5}TM$ thin films. In Figure 7, the effect of the crystallization temperature on the crystallinity is illustrated for $BL_{0.8}T$. From the relative peak intensities, information on the films' orientation is obtained. The peak intensities or widths, on the other hand, can be used as an indication of the crystallinity of the films; however, a quantitative treatment is hindered by the grain size difference with crystal orientation.

All the BL_xTM thin films (Figures 5 and 6) including the BL_xT film show *c*-axis preferential orientation, which is

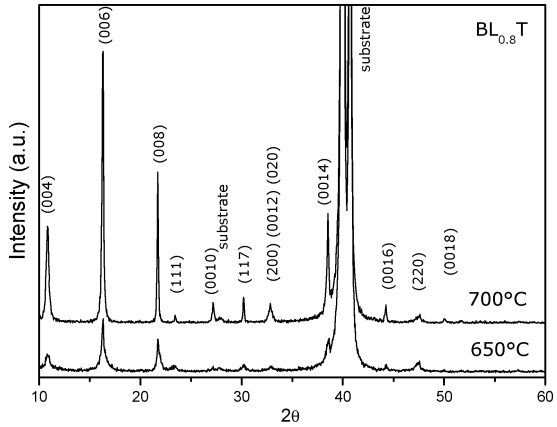

Figure 7. X-ray diffraction patterns of $BL_{0.8}TM$ thin films crystallized at different temperatures.

Table 2. Orientation Factor α for BL_xTM Thin Films Annealed at 650 or 700 °C as Indicated

	α (%)		α (%)
$BL_{0.8}TW$	66.1	$BL_{0.5}TW$	58.0
$BL_{0.8}TMo$	90.8	$BL_{0.5}TMo$	37.1
$BL_{0.8}T$	86.0	$BL_{0.5}T$	89.8
$BL_{0.8}T$ (700 °C)	92.6		
$BL_{0.8}TNb$	90.2	$BL_{0.5}TNb$	85.5
$BL_{0.8}TV$	48.8	$BL_{0.5}TV$	63.6

expected to lead to a limitation of the P_r values obtained since the largest spontaneous polarization is found along the *a*-axis in BiT. The orientation is evident from a comparison of the (006) and (117) integrated peak intensities (Table 2) by calculating the orientation factor, $\alpha = (I_{(006)}/(I_{(006)} + I_{(117)}))$,[25] which is a measure for the degree of *c*-axis orientation of the BLTM thin film. Applying this formula to the JCPDS reference (35−-0795) for bismuth titanate after correcting the intensities for thin film geometry[15] shows that an orientation factor α of 19.7% can be expected for a randomly oriented film.

The XRD patterns of the $BL_{0.8}TM$ thin films after annealing at 650 °C are shown in Figure 5. The $BL_{0.8}TV$ thin film is characterized by the smallest orientation factor (48.8%), but this is still higher than for a randomly oriented film. $BL_{0.8}TNb$ (90.2%) and $BL_{0.8}TMo$ (90.8%) both have similar α values, but they have very different peak intensities, which indicates a difference in crystallinity. This may be correlated to the large difference in these films' remanent polarization values (5.6 and 1.3 $\mu C/cm^2$, respectively) as well. For $BL_{0.8}TW$, α is relatively small (66.1%), but the observed peak intensities are very low, while the peaks are relatively wide, which indicates that the crystallites have a very small size.

In Figure 6, the XRD patterns of the $BL_{0.5}TM$ films are shown. Cosubstitution with M^{n+} leads to a decrease of the *c*-axis orientation as compared to $BL_{0.5}T$ (α = 89.5%) in all these cases. $BL_{0.5}TMo$ and $BL_{0.5}TW$ have the smallest α values (37.1 and 58%, respectively), but they also show low XRD peak intensities (Figure 6). $BL_{0.5}TNb$ is characterized by a strong *c*-axis preferential orientation (85.5%), but at the same time, it shows a very high peak intensity, as does $BL_{0.5}TV$, although with less *c*-axis preference (α = 63.6%).

Thin Film Morphology and Microstructure. The grain size and shape in the films was studied using scanning

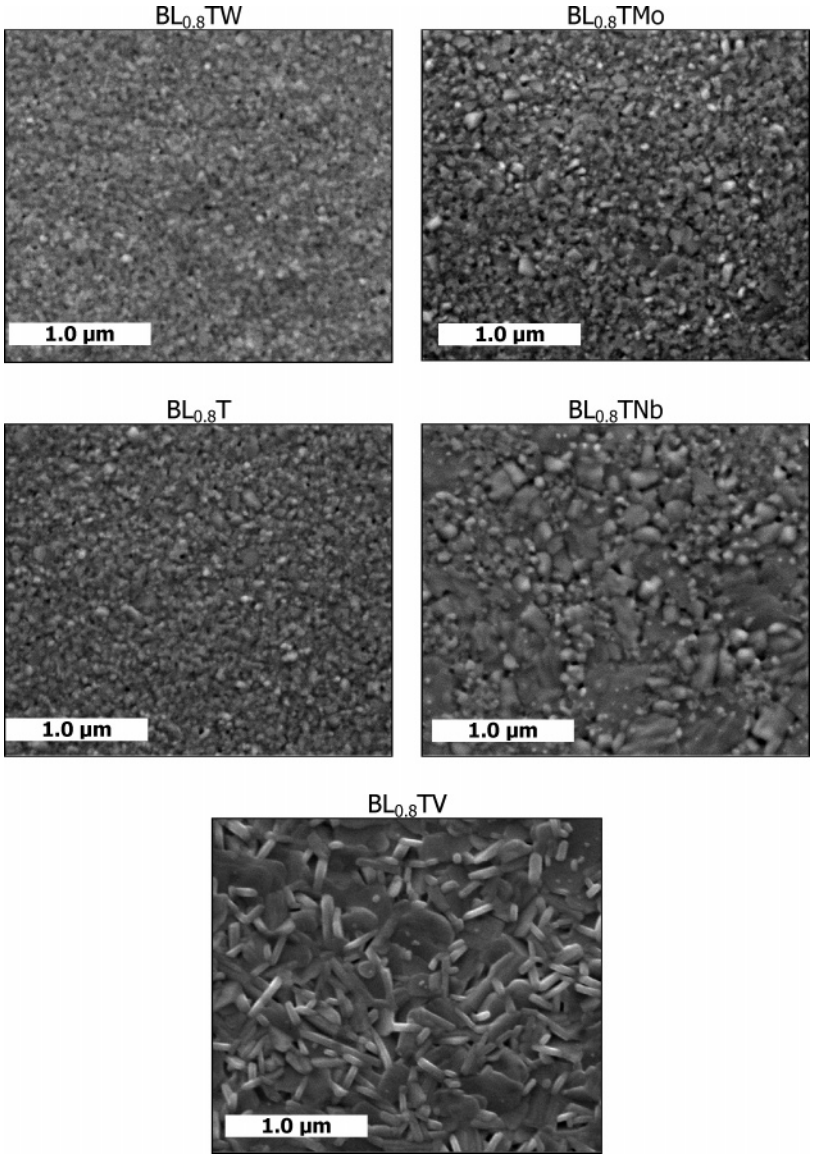

Figure 8. Secondary electron scanning electron micrographs of $BL_{0.8}TM$ thin films annealed at 650 °C in O_2, M as indicated.

electron microscopy (SEM, Figures 8−10). Grain sizes are treated qualitatively as quantification by electron backscattering diffraction (EBSD) was not possible for all of the samples due to pattern overlap caused by too small grain sizes and because EBSD only provides information for the largest grains.

The microstructure of the $BL_{0.8}TM$ thin films (Figure 8) is characterized by the presence of very small grains, except for the $BL_{0.8}TV$ and $BL_{0.8}TNb$ films. The latter show the largest grain sizes, which agrees with the observation of the largest P_r values for these compositions. For $BL_{0.8}TV$, elongated grains are observed together with large plate-like grains and rounded grains. Singh and Ishiwara also observed the presence of large plate-like grains, which were assumed to be *c*-axis oriented, as well as elongated grains for BLTNb.[21] The same grain shapes (rounded, elongated, and plate-like) are observed in the SEM images of the $BL_{0.5}TM$ thin films (Figure 9) except in the case of $BL_{0.5}TW$. The latter has the smallest grain size, consistent with $BL_{0.8}TW$. A decrease of the grain size upon substitution of bismuth titanate with W was observed by Kim et al.[28] as well.

Finally, in Figure 10, the microstructure of a $BL_{0.8}T$ film after annealing to a higher temperature of 700 °C is shown. Comparison with the $BL_{0.8}T$ film annealed at 650 °C shows a strong enhancement of grain growth with crystallization temperature, in accordance with expectations. The appearance of large, plate-like grains is observed, which are *c*-axis oriented,[14] in agreement with the increase of α (Table 2).

Discussion

Precursor Synthesis. All the (mono)metal ion precursors have to be stable against precipitation, allowing stoichiometric mixing and avoiding phase segregation. Furthermore, the design of the new aqueous precursors for M^{n+} ($n = 5$ or 6), presented here, was aimed to limit as much as possible the chemical complexity of the BLTM precursor solution, which already contains citratoperoxo complexes of Bi^{3+}, La^{3+}, and Ti^{4+}. In this way, the influence of $M^{5/6+}$ on the BLT precursor, which was optimized for stability and

(28) Kim, J. K.; Song, T. K.; Kim, S. S.; Kim, J. *Mater. Lett.* **2002**, *57*, 964.

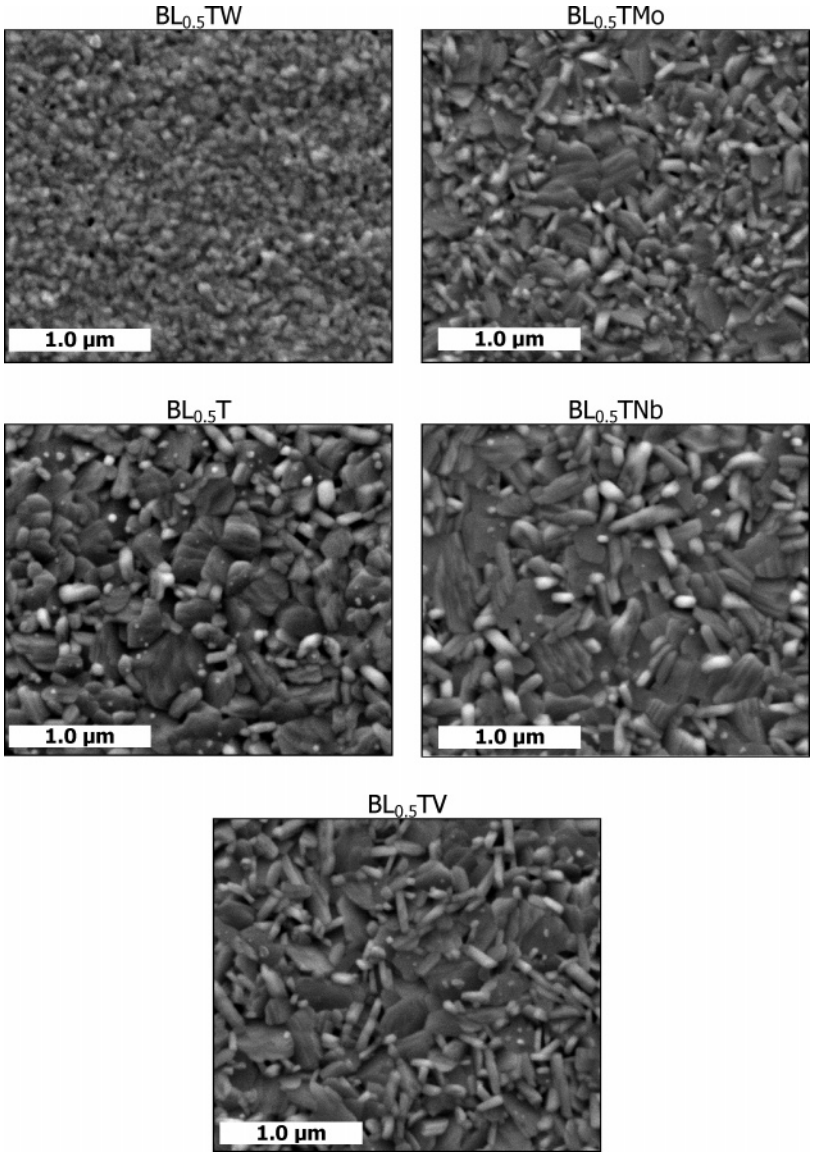

Figure 9. Secondary electron scanning electron micrographs of $BL_{0.5}TM$ thin films annealed at 650 °C in O_2, M as indicated.

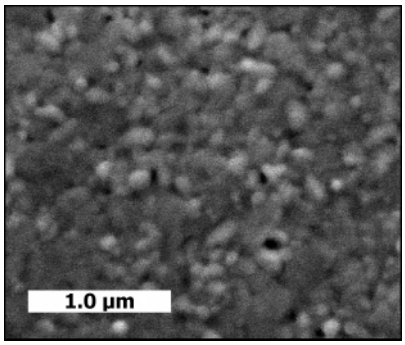

Figure 10. Secondary electron scanning electron micrographs of $BL_{0.8}T$ thin film annealed at 700 °C in O_2.

spinnability, would be minimal, allowing us to maintain the optimal precursor properties. This was obtained for La(III), Bi(III), Ti(IV), Nb(V), W(VI), and Mo(VI) by complexation with peroxo and citrato ligands after pH optimization.

The preparation of an aqueous citrato precursor solution for V^{5+} was not possible, even though the existence of crystalline citrato-oxoperoxovanadate(V) complexes with K^+ or Na^+ counterions has been shown by Djordjevic et al.[29] The observations described (gas evolution, precipitation, and color changes) indicate that H_2O_2 is decomposed and that V(V) is reduced.[30] However, it is crucial that vanadium is in the V^{5+} oxidation state for the concept of cosubstitution with higher valent metal ions to be effective. As shown, the loss of hydrogen peroxide is followed by a reduction of V(V), but this reduction depends on the heteroligand that is used.[31] A very stable complex is peroxo-aminopolycarboxylatovanadate(V): $K_2[VO(O_2)(C_6H_6NO_6)]\cdot 2H_2O$.[30] However, the KOH or NaOH that these authors used for pH adjustment was replaced by NH_3 in our work (Figure 1b), as NH_4^+ can be removed during thermal decomposition. This allows the solution to be used as a V(V) precursor for BLTV. This would not be possible with Na^+ and K^+, as these would affect the film's electrical properties upon their incorporation into the crystal lattice of BLTM or upon formation of secondary phases. As a conclusion from the results on the V^{5+}

(29) Djordjevic, C.; Lee, M.; Sinn, E. *Inorg. Chem.* **1989**, *28*, 719.
(30) Djordjevic, C.; Wilkins, P. L.; Sinn, E.; Butcher, R. J. *Inorg. Chim. Acta* **1995**, *230*, 241.
(31) Djordjevic, C.; Leerenslo, M.; Sinn, E. *Inorg. Chim. Acta* **1995**, *233*, 97.

precursor's stability, its gelation by evaporation in the furnace and the gel's thermal decomposition into the oxide, it is shown that the nitrilotriacetatoperoxoV(V) complex is stable against reduction during all of these stages. Therefore, it is concluded that this precursor is suitable for the incorporation of V(V) into BLT.

Thin Film Characterization. Ferroelectric Hysteresis Loops. Of all the BLTM compositions studied in this work, the BLTV showed the highest P_r value, both for $x = 0.8$ (7.0 μC/cm^2) and $x = 0.5$ (8.6 μC/cm^2). These values can be compared to literature values (e.g., refs 23, 28, 32, and 33); however, the comparison is troubled by differences in crystallization temperature, film thickness, and applied voltage amplitude. In any case, the reported values can be considered to be of good quality, certainly in view of the limited thermal budget (650 °C).

There is a much larger remanent polarization obtained for the $BL_{0.5}$TM films than for the corresponding $BL_{0.8}$TM films as is clear from Table 1. The effect of the amount of La^{3+} on the properties of BLT films deposited without cosubstitution using the aqueous solution−gel route is related to a grain growth inhibition effect of La^{3+}.[25] A smaller grain size implies an increased number of grain boundaries, which can have a pinning effect on the remanent polarization.

The increase of the P_r value upon introduction of M^{n+} into the crystal structure is ascribed to two different contributions. First, there is a decrease of the oxygen vacancy concentration when doping with higher valent metal ions than Ti^{4+}. Second, possibly a structural distortion exists in the TiO_6 octahedron of the crystal lattice, due to the difference in ionic radius between, for instance, Ti^{4+} and Nb^{5+}. As a result, there is an enhanced possibility for ion displacement, which could be another reason for an improvement of the polarization characteristics.[21] However, if only these effects were involved, W(VI) and Mo(VI) should also lead to improved P_r values, which is in contrast with the present observations. As the ferroelectric properties are also influenced to a great extent by the thin film microstructure and by the presence of possible secondary phases or preferential orientation, these characteristics were studied using scanning electron microscopy (SEM) and X-ray diffraction (XRD) to explain the apparent discrepancy.

Crystal Structure: XRD. It is clear (Figures 5 and 6) that the BL_xTM films contain a single phase. There is no evidence for phase segregation of any of the individual metal ions, which would lead to the formation of secondary (mono)metal oxide phases. The diffraction peak positions in the BLTM films are practically identical to the peak positions for the JCPDS reference of bismuth titanate. This indicates that the substitution with higher valent metal ions has a limited effect on the lattice parameters of the BL_xTM thin films, which can be ascribed to the very small quantities of high valent metal ions substituting for Ti^{4+}.[34] No direct correlation between the orientation factor α and the P_r value could be demonstrated. This can be ascribed to an added contribution of the film's crystallinity and microstructure, which interferes with the effect of the crystallite orientation. This will be discussed in the next paragraph.

As compared to the $BL_{0.8}$TM films, the $BL_{0.5}$TM thin films show more intense and narrower peaks, indicating a larger crystallite size.[25] Here, this effect is suggested to be one of the reasons for the increase of the remanent polarization value when comparing $BL_{0.5}$TM with $BL_{0.8}$TM as well.

After annealing $BL_{0.8}$T at 700 °C, there is a slight increase of the orientation factor as is shown in Table 2. A higher annealing temperature leads to a larger crystallite size or improved crystallinity, as is derived from the appearance of narrower and more intense peaks upon crystallizing the $BL_{0.8}$T film at 700 °C (Figure 7). Both of these observations together indicate that there is grain growth upon annealing to a higher temperature, which is favored in the *c*-direction as compared to the other crystal planes. Grain growth is expected to be enhanced by higher annealing temperatures due to the increased ion mobility. The grain growth also explains the P_r improvement after crystallizing the films at higher temperatures. A decrease of P_r with decreasing grain size has been described in the literature for ferroelectric ceramics as well as thin films.[35−41] It can be ascribed to domain pinning at the grain boundaries and the reduction of the number of different domain configurations both leading to a reduction of the domain wall mobility as well as the number of domains that can be switched. Finally, additional pinning of domain walls is due to the reduction of stress relief by ferroelectric domain formation in small sized grains.

The increase of the orientation factor with the crystallization temperature indicates a texture development, which can be ascribed to abnormal grain growth. This is caused by an anisotropic grain surface free energy, which is related to the crystallographic orientation of the grain. It appears that the grains with a *c*-axis orientation have a lower surface free energy, which is advantageous to their growth. As the films are thin (120 nm), this becomes an important effect.[42] The preference for *c*-axis orientation that is observed in substituted bismuth titanate films is not determined by the substrate, as there is no good lattice matching with the Pt(111) substrate. However, the development of a preferential *c*-axis orientation can be ascribed to the preferential crystal growth along the crystal planes perpendicular to the *c*-axis, due to their lower surface free energy.[42,43] The strong

(32) Bao, Z. H.; Yao, Y. Y.; Zhu, J. S.; Wang, Y. *Mater. Lett.* **2002**, *56*, 861.
(33) Uchida, H.; Okada, I.; Matsuda, H.; Iijima, T.; Watanabe, T.; Funakubo, H. *Jpn. J. Appl. Phys.* **2004**, *43*, 2636.
(34) Noguchi, Y.; Miyayama, M. *Appl. Phys. Lett.* **2001**, *78*, 1903.
(35) Ren, S. B.; Lu, C. J.; Liu, J. S.; Shen, H. M.; Wang, Y. N. *Phys. Rev. B* **1996**, *54*, 14337.
(36) Cao, W. W.; Randall, C. A. *J. Phys. Chem. Solids* **1996**, *57*, 1499.
(37) Damjanovic, D.; Demartin, M. *J. Phys.: Condens. Matter* **1997**, *9*, 4943.
(38) Ren, S. B.; Lu, C. J.; Shen, H. M.; Wang, Y. N. *Phys. Rev. B* **1997**, *55*, 3485.
(39) Chou, H. Y.; Chen, T. M.; Tseng, T. Y. *Mater. Chem. Phys.* **2003**, *82*, 826.
(40) Sakabe, Y.; Yamashita, Y.; Yamamoto, H. *J. Eur. Ceram. Soc.* **2005**, *25*, 2739.
(41) Buscaglia, M. T.; Viviani, M.; Buscaglia, V.; Mitoseriu, L.; Testino, A.; Nanni, P.; Zhao, Z.; Nygren, M.; Harnagea, C.; Piazza, D.; Galassi, C. *Phys. Rev. B* **2006**, *73*.
(42) Thompson, C. V. *Annu. Rev. Mater. Sci.* **1990**, *20*, 245.
(43) Chen, Y. C.; Sun, Y. M.; Lin, C. P.; Gan, J. Y. *J. Cryst. Growth* **2004**, *268*, 210.

variation of the composition along the *c*-axis necessitates a strong diffusion for growth to occur.[44]

Thin Film Morphology and Microstructure. From a comparison of $BL_{0.8}TM$ (Figure 8) and $BL_{0.5}TM$ (Figure 9), it immediately becomes clear that there is an overall difference in the grain size, which is consistent with the conclusions from the XRD study and correlates with the amount of La^{3+} substituted for Bi^{3+}. This difference is ascribed to a grain growth inhibition effect of La^{3+}, which has a lower ion mobility as compared to Bi^{3+}, in thin films deposited from aqueous CSD.[25]

Furthermore, the results show that Mo^{6+} and especially W^{6+} seem to behave as grain growth inhibitors. It appears that Nb^{5+} simply enhances the abnormal grain growth, without changing the free surface energy of the grain, leading to an increase of the *c*-axis preferential orientation.[42] On the contrary, V^{5+} seems to affect grain growth in a different way. Here, the significant decrease of the *c*-axis preferential orientation seems to indicate that V^{5+} changes the free surface energy of the grains, leading to a less enhanced growth of the *c*-axis oriented grains.[42]

Conclusion

An original, entirely aqueous route for the synthesis of ferroelectric $(Bi,La)_4(Ti,M)_3O_{12}$ ($M^{n+} = W^{6+}$, Mo^{6+}, V^{5+}, or Nb^{5+}) has been developed and successfully applied to the deposition of ferroelectric thin films on platinized substrates.

There are several influences that need to be taken into account when explaining the remanent polarization of BLTM thin films deposited using this aqueous chemical solution deposition method. First of all, the effect of the substituents is important on the level of point defects in the crystal structure of the material. Second, the grain size, or the film's morphology and its microstructure, need to be considered. Finally, the orientation of the crystallites relative to the substrate, the film's texture, is of great importance as well. By combining X-ray diffraction and scanning electron microscopy, information on these factors was acquired. This led to a solid basis for the explanation of trends in the ferroelectric properties of thin films from the aqueous solution−gel route. The influence of cosubstitution with higher valent metal ions on the number of oxygen vacancies appears to be dominated by the effects of grain growth inhibition and *c*-axis preferential orientation. When cosubstitution led to enhanced grain growth, as for BLTNb, or when a reduced *c*-axis preferential orientation was observed, as for BLTV, an improved P_r value was observed. A decreased grain growth, however, as in the case for BLTW, led to a limitation of the P_r value, in spite of a positive texture effect.

Generally, the aqueous solution−gel route presented here is believed to be suitable for the preparation of other multimetal oxides with complex compositions as well, allowing for a number of ecologic, economic, and practical advantages.

Acknowledgment. A.H. and M.K.V.B. are post-doctoral research fellows of the Research Foundation Flanders (FWO-Vlaanderen). This research was partly performed in the framework of the Projects 1.2.16/D2/841 and 1.2.14/PO/841 of the Objective 2 Program for Limburg (Belgium) of the European Regional Development Fund under "Integrated Material Research for Development and Application in the Automotive Sector".

CM070101X

(44) Chen, Y. C.; Sun, Y. M.; Lin, C. P.; Gan, J. Y. *J. Crys. Growth*, **2004**, *268*, 210.